Fuel Economy Analysis of Periodic Cruise Control Strategies for Power-Split HEVs at Medium and Low Speed

Conference Paper · April 2018

DOI: 10.4271/2018-01-0871

CITATIONS
0

READS
259

6 authors, including:

Qingfeng Lin
Beihang University (BUAA)
20 PUBLICATIONS **92** CITATIONS
SEE PROFILE

Shaobing Xu
Tsinghua University
12 PUBLICATIONS **151** CITATIONS
SEE PROFILE

Shengbo Eben Li
Tsinghua University
160 PUBLICATIONS **3,512** CITATIONS
SEE PROFILE

2018-01-0871 Published 03 Apr 2018

Fuel Economy Analysis of Periodic Cruise Control Strategies for Power-Split HEVs at Medium and Low Speed

Qingfeng Lin and Xuedong Liu Beihang University

Xiaoxue Zhang China Agricultural University

Zhitao Wang Tsinghua University

Shaobing Xu University of Michigan

Shengbo Li Tsinghua University

Citation: Lin, Q., Liu, X., Zhang, X., Wang, Z. et al., "Fuel Economy Analysis of Periodic Cruise Control Strategies for Power-Split HEVs at Medium and Low Speed," SAE Technical Paper 2018-01-0871, 2018, doi:10.4271/2018-01-0871.

Abstract

Hybridization of vehicles is considered as the most promising technology for automakers and researchers, facing the challenge of optimizing both the fuel economy and emission of the road transport. Extensive studies have been performed on power-split hybrid electric vehicles (PS-HEVs). Despite of the fact that their excellent fuel economy performance in city driving conditions has been witnessed, a bottle neck for further improving the fuel economy of PS-HEVs has been encountered due to the inherent engine-generator-motor power circulation of the power-split system under medium-low speed cruising scenarios. Due to the special mechanical constraints of the power-split device (PSD), the conventional periodic cruising strategy like Pulse and Glide cannot be applied to PS-HEVs directly. To further realize the fuel economy potential of PS-HEVs, in this paper, two different periodic cruising strategies are presented, namely three-phase strategy and two-phase strategy, and their optimized output power in each phase are identified by solving an optimization problem. By comparing with a constant speed cruising strategy, a significant improvement can be observed and the effectiveness of the proposed cruising strategies is validated. Finally, the underlying fuel-saving mechanism of the periodic strategies is discussed.

Introduction

Due to good fuel economy and emission performance, hybrid electric vehicles (HEVs) have been widely accepted by consumers during the past two decades. A typical HEV is equipped with at least two different power sources - gasoline engine and electrochemical battery [1,2]. According to the structure of the powertrain system, HEV can be mainly divided into three categories: series, parallel and power-split. The power-split HEV (PS-HEV) is the most popular one capturing almost 80% HEV market share. Unlike series and parallel HEVs, PS-HEV uses a planetary gear set as the power split device (PSD). The power from the engine can be distributed into the battery or used to drive the vehicle wheels via the PSD. Therefore, PS-HEV has better flexibility and fuel economy but its structure and control mechanism are more complex than the other two categories [3]. The advantages of the PS-HEV with PSD include: 1). Engine speed can be decoupled from the wheel speed. 2). Low-efficiency engine operations can be avoided by adjusting electric motor operations. 3). Kinetic energy can be reclaimed by the regenerative braking system [4].

The fuel economy of PS-HEV depends on not only powertrain configurations but also vehicle control strategies [2]. In addition to improving component efficiency, optimizing vehicle speed to match with environmental constraints and vehicle's nonlinear operation characteristics can also reduce fuel consumption by 5~20%, which is known as the economic driving technique [5]. A typical economic driving technique is called Pulse and Glide (PnG).

PnG strategy is a dynamic cruising strategy with two phases; the first phase is called the pulse (or acceleration) phase, drivers or control systems need to accelerate the vehicle from a lower speed to a higher speed. Then the vehicle transitions to the second phase - the glide (or coasting) phase, the vehicle coasts to a lower speed, with an average speed equal to the expected velocity [6]. Compared to the constant speed strategy (CS), PnG requires periodical fluctuations on vehicle speed and dynamic controls on engine and transmission. Although this strategy has great potential to reduce fuel consumption, not all accelerating operations can achieve the goal of fuel saving [7]. The dynamic control inputs, i.e., engine torque output and gear position, should be carefully determined.

Improper control inputs, e.g., following the qualitative tips like "slow accelerations", may even cause more fuel consumption than CS [8]. The engine fuel consumption rate is not strictly linear regarding to the output power. As shown in Figure 1, there is a local turning-point of fuel consumption at medium power, called the sweet spot. The main idea of PnG is that the engine first operates at the sweet spot to pulse the vehicle, then switches to shut down (or idle) point in glide phase. The speed profile and engine fuel injection rate are shown in Figure 1.

Several studies have presented the applications of the periodic strategies and its fuel-saving mechanism on conventional vehicles over the last few years. For vehicles with continuously variable transmission (CVT), Li and Peng optimized the PnG strategy under an optimal control framework. For the particular vehicle/engine they studied, it was found that depending on the vehicle speed, the best strategy can vary from PnG to CS [7]. The speed-dependent behaviour arises from the nonlinear characteristics of internal combustion engine. Up to 20% of fuel can be saved by periodic control [6]. Xu and Li proposed a suboptimal but practical PnG strategy for vehicles with step-gear transmission [7]. They also studied PnG operation for parallel HEVs and divided the optimal operation under different speed constraints into two subtypes: Speed-PnG and SoC-PnG, and proved that V-PnG is the most efficient operation which can avoid energy conversion loss between battery and motors [8]. Li and his colleagues have presented a periodic servo-loop controller for a chain of multiple connected vehicles to minimize the overall fuel consumption, in which a sectional switching map is used to select either pulse phase or glide phase according to current inter-vehicle states [9,10].

Different from conventional vehicles or parallel HEV, the PS-HEVs have a special mechanical design-the motor, engine and vehicle motion are coupled with each other by the PSD. If the PnG strategy is applied, PS-HEV's mechanical design will compel the generator to charge the battery when the engine is accelerating the vehicle. Thus, the battery will be fully charged after hundreds of PnG cycles, and then the PnG operation will be forced to exit. Therefore, PnG strategy cannot be directly applied to the PS-HEV considering SoC sustainability.

To solve this problem, this paper presents two different periodic control strategies based on the operation of electric motors. The periodic cruising problem is first transformed into an optimization problem, and solved using nonlinear programming. Furthermore, the effectiveness of the proposed strategies is verified by comparing them with constant speed cruising strategy.

FIGURE 1 Pulse and Glide operation for conventional ICE vehicles

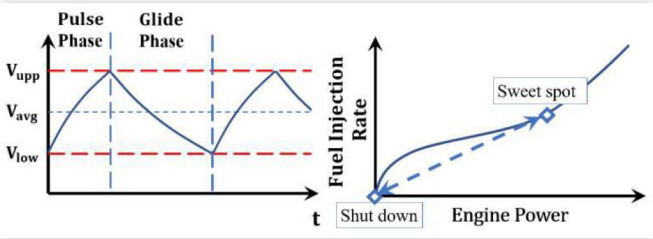

This paper is organized as follows: first, a general description of a PS-HEV model and problem statement is presented; second, the optimization results of the problem are described in detail, including the performance of different control strategies; finally, the fuel-saving mechanisms of the proposed strategies are proven by system efficiency analyses.

PS-HEV Modelling and Problem Statement

The PS-HEV studied here is a typical single mode power split system, equipped with a 2.0 L Atkinson cycle gasoline engine, two permanent magnet DC motors, namely MG 1 and MG 2, an engine lock, a power split device (PSD), a Lithium battery pack and a reducer. Its architecture is shown in Figure 2.

With the mechanical structure, the PS-HEV has several driving modes. Some of those used in this paper are described as follows:

- Pulsing: The PSD splits the engine power into two parts: accelerating the vehicle and charging the battery by MG 1.
- Pure electric cruising: ICE shuts down and immobilized by a lock while MG 2 alone uses battery power to drive the vehicle.
- Free gliding: No power source is engaged, and the engine(ICE) is immobilized by the lock; therefore, the vehicle speed is being decreased only by road and air resistance; and there is no regeneration operation during this process.
- EV-mode gliding: Different from the aforementioned free gliding. MG 2 provides a small amount of torque to extend the gliding process, with the engine and the MG 1 turned off.

As previously mentioned, when constrained by planetary gearset, applying a high engine power in the pulse phase will increase both vehicle speed and battery SoC.

To achieve a sustainable battery SoC, two different glide(discharge) modes are proposed: 1) vehicle speed and the

FIGURE 2 A typical PS-HEV architecture with a single planetary gearset

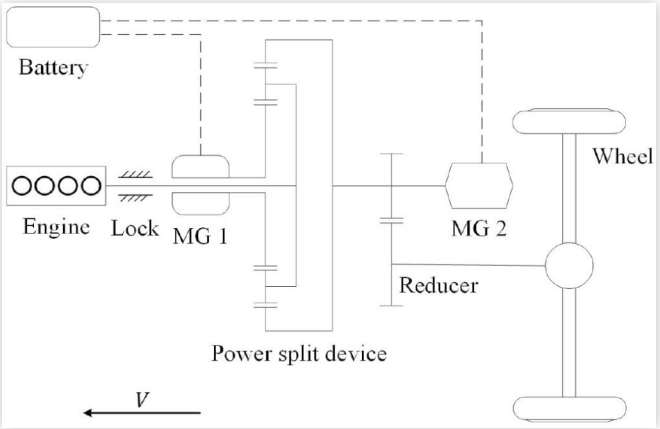

FIGURE 3 The two periodic cruising strategies for PS-HEVs

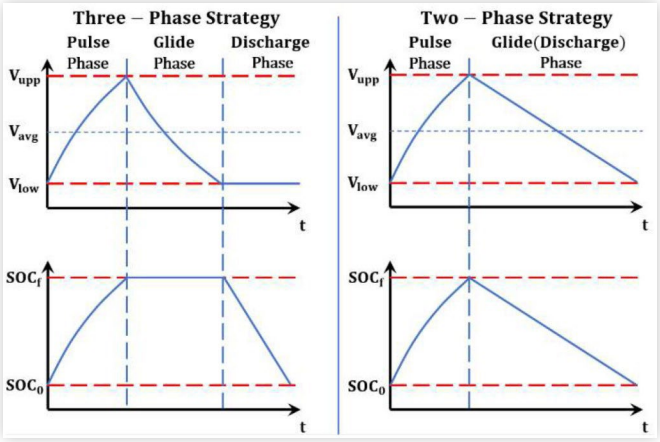

battery SoC sequentially declining to their initial state, and the corresponding mode switching is: Pulsing-Free gliding-Pure electric cruising; 2) vehicle speed and the battery SoC simultaneously declining to their initial values, and its mode switching is: Pulsing-EV-mode gliding. According to their numbers of phases, the two strategies are named "Three-Phase strategy" and "Two-Phase Strategy" respectively, and their vehicle speed and battery SoC profiles are shown in Figure 3.

For periodic cruising strategies, engine and motor operations in the pulse phase are optimized to achieve an optimal fuel economy; any arbitrary operation may lead to a worse fuel economy. The main purpose of this paper is to determine the optimal periodic cruising strategy for PS-HEVs, that is, finding the optimal engine and motor operations to improve the fuel economy.

PS-HEV Dynamics

Since the recovery efficiency of the regenerating system is not 100%, leading to a considerable energy loss for a long travel, while the energy releasing efficiency of the vehicle body can achieve 100% [8]. In this paper, we assumed that the regenerating system is switched off during gliding, and the vehicle is only being decelerated by road and air resistance in order to pursue the maximum energy efficiency.

Besides, to keep the problem simple, the following assumptions are made:

- The engine operation point is kept stable when vehicle is accelerating or cruising;
- The dynamic processes of engine start/stop are ignored, in other words, assuming the operations of engine start/stop can be completed instantly;
- Electrical appliances such as air conditioner are all turned off, so the changes of battery SoC are only caused by the operations of the MG 1 and MG 2.

Based on the above assumptions, a PS-HEV model is constructed and a corresponding problem can be formulated.

The dynamic equations of motion of PS-HEV can be expressed with a matrix equation as the following [11,12]:

$$\begin{bmatrix} I_r + I_{MG2} + m\frac{R_w^2}{K^2} & 0 & 0 & -R \\ 0 & I_c + I_{eng} & 0 & R+S \\ 0 & 0 & I_s + I_{MG1} & -S \\ -R & R+S & -S & 0 \end{bmatrix} \begin{bmatrix} \dot{\omega}_{out} \\ \dot{\omega}_{eng} \\ \dot{\omega}_{MG1} \\ F \end{bmatrix} = \begin{bmatrix} T_{MG2} - T_{load} \\ T_{eng} \\ T_{MG1} \\ 0 \end{bmatrix} \quad (1)$$

$$T_{load} = \frac{R_w}{K}\left[mgf + \frac{1}{2} C_D A_f \rho_{air} (V)^2 \right] \quad (2)$$

$$V = \frac{R_w}{K}\omega_{out} \quad (3)$$

where I_s, I_c, I_r, I_{MG1}, I_{MG2} and I_{eng} are rotational inertia of the sun gear, carrier, ring gear, MG 1 rotor, MG 2 rotor and the engine crankshaft, respectively. T_{MG1}、T_{MG2}、T_{eng} are torque of the MG 1, MG 2 and the engine. $\dot{\omega}_{MG1}$, $\dot{\omega}_{eng}$, $\dot{\omega}_{out}$ are angular acceleration of the MG 1, MG 2 and the output shaft. F is the internal force between different gears. m is the vehicle mass. R_w is the tyre radius. K is the final ratio. g is the gravitational constant. f is the rolling resistance coefficient. C_D is the drag coefficient. A_f is the vehicle frontal area. ρ_{air} is the air density. V is the vehicle speed.

Set the vehicle dynamics property matrix as $\boldsymbol{D}$:

$$\boldsymbol{D} = \begin{bmatrix} I_r + I_{MG2} + m\frac{R_w^2}{K^2} & 0 & 0 & -R \\ 0 & I_c + I_{eng} & 0 & R+S \\ 0 & 0 & I_s + I_{MG1} & -S \\ -R & R+S & -S & 0 \end{bmatrix} \quad (4)$$

Then vehicle's dynamics can be obtained by:

$$\begin{bmatrix} \dot{\omega}_{out} \\ \dot{\omega}_{eng} \\ \dot{\omega}_{MG1} \\ F \end{bmatrix} = \boldsymbol{D}^{-1} \begin{bmatrix} T_{MG2} - T_{load} \\ T_e \\ T_{MG1} \\ 0 \end{bmatrix} \quad (5)$$

The dynamics of the output shaft and the engine can be obtained by drawing the first two rows of the matrix equation above:

$$\dot{\omega}_{out} = D_{11}^{-1} \cdot \left(T_{MG2} - T_{load}\right) + D_{12}^{-1} \cdot T_{eng} + D_{13}^{-1} \cdot T_{MG1} \quad (6)$$

$$\dot{\omega}_{eng} = D_{21}^{-1} \cdot \left(T_{MG2} - T_{load}\right) + D_{22}^{-1} \cdot T_{eng} + D_{23}^{-1} \cdot T_{MG1} \quad (7)$$

where D_{ij}^{-1} is the entry located in i^{th} row j^{th} column in the $\boldsymbol{D}$'s inverse matrix $\boldsymbol{D^{-1}}$.

Since the ring gear is linked to the output shaft, they have the same rotation speed. To make the results more intuitive, the output shaft speed is converted into the vehicle speed:

$$\dot{V} = \frac{R_w}{K}\left[D_{11}^{-1} \cdot \left(T_{MG2} - T_{load}\right) + D_{12}^{-1} \cdot T_{eng} + D_{13}^{-1} \cdot T_{MG1} \right] \quad (8)$$

FIGURE 4 Efficiency map of the MG 1 and MG 2

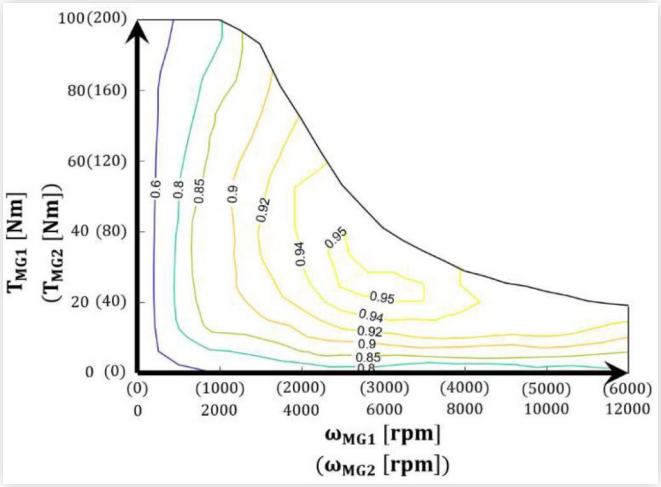

Moreover, an internal resistance battery model is used in this paper, which can be expressed by:

$$\dot{SoC} = -\frac{V_{oc} - \sqrt{V_{oc}^2 - 4P_b \times R_{int}}}{2R_{int} \times C} \tag{9}$$

where SoC is the battery state of charge, V_{oc} is the open circuit voltage, R_{int} is the internal resistance, C is the battery capacity, P_b is the battery power, which is described by:

$$P_b = \omega_{out} T_{MG2} \eta_{MG2}^{p} + \omega_{MG1} T_{MG1} \eta_{MG1}^{q} \tag{10}$$

If MG 2 is operating in drive mode, then $p = 1$, otherwise $p = -1$; If MG 1 is running in drive mode, then $q = 1$, otherwise $q = -1$.

Efficiencies of the MG 1 η_{MG1} and MG 2 η_{MG2} are described with a same map, as shown in Figure 4.

The motor efficiency η_{MG} is a function of motor speed ω_{MG} and motor torque T_{MG}, fitted by a bivariate polynomial:

$$\eta_{MG} = \sum_{i=0}^{5}\sum_{j=0}^{i} A_{1+j+\sum_0^i i} \cdot \left(\frac{\omega_{MG}}{\omega_{MG\_\max}}\right)^{i-j} \cdot \left(\frac{T_{MG}}{T_{MG\_\max}}\right)^{j} \tag{11}$$

where A_is are the fitting coefficients. ω_{MG_max} and T_{MG_max} are the maximum motor speed and maximum motor torque.

Assuming that generating efficiency of the motor equals to the drive efficiency under the same torque and speed, i.e.,

$$\eta_{gen}\left(-T_{gen}, \omega_{gen}\right) = \eta_{mot}\left(T_{mot}, \omega_{mot}\right) \tag{12}$$

Performance Index

The fuel consumption per distance unit is adopted as the performance index, which is expressed by:

$$J = \frac{\int_0^{t_f} F_e dt}{S_f} \tag{13}$$

where t_f, F_e, and S_f are the final time, the engine fuel injection rate, and the terminal distance of a single cycle, respectively.

FIGURE 5 The BSCF map of the engine

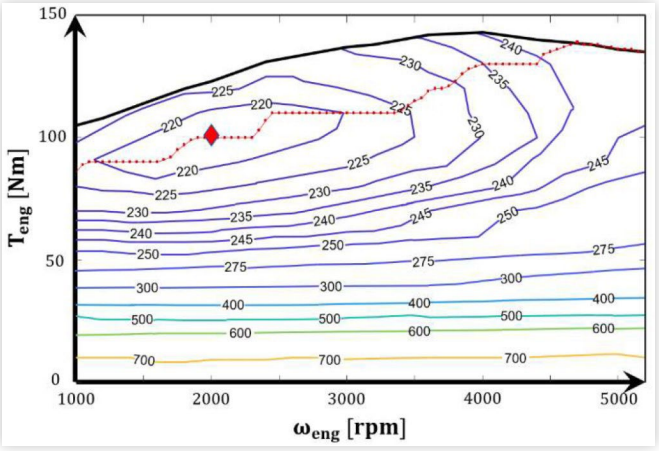

The engine fuel injection rate F_e is defined as:

$$F_e = B_e\left(T_{eng}, \omega_{eng}\right) \cdot \left(T_{eng} \cdot \omega_{eng}\right) \tag{14}$$

where B_e is the BSFC of the engine, which is a function of engine speed ω_{eng} and engine output torque T_{eng}. It is set to zero if the engine is shut down or the vehicle is gliding.

The engine BSFC map is shown in Figure 5. The point with the minimum BSFC, i.e., sweet spot which is marked with a red diamond, locates at around 2000 rpm and 100 Nm. The red dotted line is the optimal efficiency curve, and the black solid line is the maximum torque line.

Similar to motor efficiency, the engine fuel injection rate F_e can be fitted by a polynomial:

$$F_e = \sum_{i=0}^{4}\sum_{j=0}^{i} B_{1+j+\sum_0^i i} \cdot \omega_{eng}^{i-j} \cdot T_{eng}^{j} \tag{15}$$

where B_i are the fitting coefficients.

Constraints Sets

Constraints are mainly derived from the physical limits of the powertrain components. Moreover, to avoid excessively charging or discharging the battery, SoC is maintained within a predefined range:

$$0 \le T_{eng} \le T_{eng,\max}\left(\omega_{eng}\right)$$

$$0 \le \omega_{eng} \le \omega_{eng,\max}$$

$$T_{MG2,\min}\left(\omega_{MG2}\right) \le T_{MG2} \le T_{MG2,\max}\left(\omega_{MG2}\right)$$

$$T_{MG1,\min}\left(\omega_{MG1}\right) \le T_{MG1} \le T_{MG1,\max}\left(\omega_{MG1}\right)$$

$$\omega_{MG2,\min} \le \omega_{MG2} \le \omega_{MG2,\max}$$

$$\omega_{MG1,\min} \le \omega_{MG1} \le \omega_{MG1,\max}$$

$$SoC_{\min} \le SoC \le SoC_{\max} \tag{16}$$

where the maximum torque of the engine $T_{eng,\,max}$ and motor $T_{MG,\,max}$ are related to their speed ω_{eng} and ω_{MG}:

$$T_{eng,\max}\left(\omega_{eng}\right)=\sum_{i=0}^{5}M_i\cdot\omega_{eng}^{i} \tag{17}$$

$$T_{MG1,\max}\left(\omega_{MG1}\right)=\begin{cases}100N\cdot m & 0<\omega_{MG1}<2000rpm\\ \sum_{i=0}^{3}N_i\cdot\omega_{MG1}^{i} & 2000rpm<\omega_{MG1}<12000rpm\end{cases} \tag{18}$$

$$T_{MG2,\max}\left(\omega_{MG2}\right)=\begin{cases}200N\cdot m & 0<\omega_{MG2}<1000rpm\\ \sum_{i=0}^{3}Q_i\cdot\omega_{MG2}^{i} & 1000rpm<\omega_{MG2}<6000rpm\end{cases} \tag{19}$$

where M_i、 N_i and Q_i are fitting coefficients.

To ensure the sustainability of PnG operation, both the initial and final values of vehicle-speed/battery-SoC are set to equal values:

$$V_0=V_f$$
$$SoC_0=SoC_f \tag{20}$$

Optimization Problem

The fuel-optimal periodic cruising problem of the PS-HEV is formulated as:

$$\min J=\frac{\int_0^{t_f}F_e dt}{S_f}$$

s.t.

$$\dot{V}=\frac{R_w}{K}\left[D_{11}^{-1}\cdot\left(T_{MG2}-T_{load}\right)+D_{12}^{-1}\cdot T_{eng}+D_{13}^{-1}\cdot T_{MG1}\right]$$

$$\dot{\omega}_{eng}=D_{21}^{-1}\cdot\left(T_{MG2}-T_{load}\right)+D_{22}^{-1}\cdot T_{eng}+D_{23}^{-1}\cdot T_{MG1}$$

$$\dot{SoC}=-\frac{V_{oc}-\sqrt{V_{oc}^2-4P_b\times R_{int}}}{2R_{int}\times C}$$

$$P_b=\omega_{out}T_{MG2}\eta_{MG2}^{p}+\omega_{MG1}T_{MG1}\eta_{MG1}^{q}$$

$$0\le T_{eng}\le T_{eng,\max}\left(\omega_{eng}\right)$$

$$0\le\omega_{eng}\le\omega_{eng,\max}$$

$$T_{MG2,\min}\left(\omega_{MG2}\right)\le T_{MG2}\le T_{MG2,\max}\left(\omega_{MG2}\right)$$

$$T_{MG1,\min}\left(\omega_{MG1}\right)\le T_{MG1}\le T_{MG1,\max}\left(\omega_{MG1}\right)$$

$$\omega_{MG2,\min}\le\omega_{MG2}\le\omega_{MG2,\max}$$

$$\omega_{MG1,\min}\le\omega_{MG1}\le\omega_{MG1,\max}$$

TABLE 1 Parameters of the vehicle

Vehicle Mass m	1600 kg
Drag Coefficient C_D	0.3
Frontal Area A_f	2.3 m^2
Rolling Resistance Coefficient f	0.01
Tire Radius R_w	0.301 m
Inertia of the Engine I_{eng}/MG 1 I_{MG1}/MG 2 I_{MG2}	0.26 / 0.022 / 0.04 kg/m^2
Inertia of the Ring I_r/Carrier I_c/ Sun gear I_s	0.01 / 0.008/ 0.0015 kg/m^2
Final Drive Ratio K	4.113
Battery Capacity C	1.35 kw·h
Radius of the Ring R and Sun gear S	0.26 / 0.1 m
Maximum Speed of MG 1 $\omega_{MG1,\,max}$/MG 2 $\omega_{MG2,\,max}$	10000 (MG 1)/6000 (MG 2) rpm
Minimum Speed of MG 1 $\omega_{MG1,\,min}$/MG 2 $\omega_{MG2,\,min}$	–10000 (MG 1)/0 (MG 2) rpm
Sweet Spot of the Engine	100 Nm@2000 rpm

$$SOC_{\min}\le SOC\le SOC_{\max}$$
$$V_0=V_f$$
$$SoC_0=SoC_f \tag{21}$$

The variables to be optimized are the speed and torque of each power source, i.e., T_{eng}, ω_{eng}, T_{MG1}, ω_{MG1}, T_{MG2}, ω_{out}. In order to acquire the optimization results of this nonlinear problem, it is transformed into a nonlinear programming problem and solved by SNOPT, which employs sequence quadratic programming (SQP) algorithm to obtain the results [13]. The engine map, MG efficiency map and vehicle parameters used in this paper come from a real HEV vehicle, and the main vehicle parameters are listed in Table 1:

Optimization Results

In order to illustrate the optimization results of different strategies, three speeds as following are considered: 20 km/h, 40 km/h and 60 km/h, and the speed fluctuation value is ±5 km/h in the periodic strategies. i.e., $V_{min}=V_{avg}-5km/h$, $V_{max}=V_{avg}+5km/h$.

Constant Speed Strategy-Benchmark

In this paper, the constant speed strategy is used as a benchmark to verify periodic cruising strategy's fuel-saving effects.

The constant speed strategy is divided into two phases, namely charge phase and discharge phase while the upper and lower SoC boundaries are set to 0.6 and 0.4 respectively. The first phase consists of engine propulsion and MG 1 power generation, where vehicle speed is kept stable and battery SoC has a positive gain. The second phase consists of pure electric driving, that the engine is in shut down mode, and the vehicle

FIGURE 6 Optimization results of constant speed strategy under sample speed

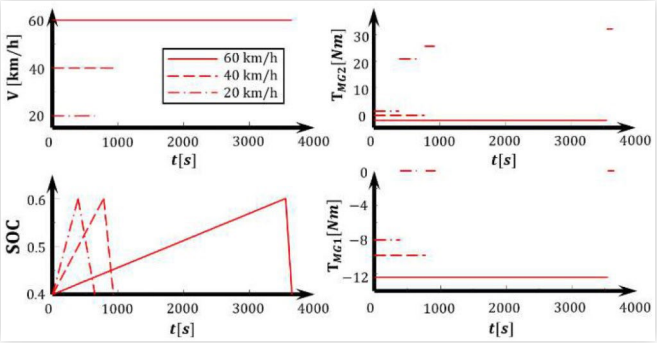

FIGURE 7 Optimization results of three-phase strategy under sample speeds

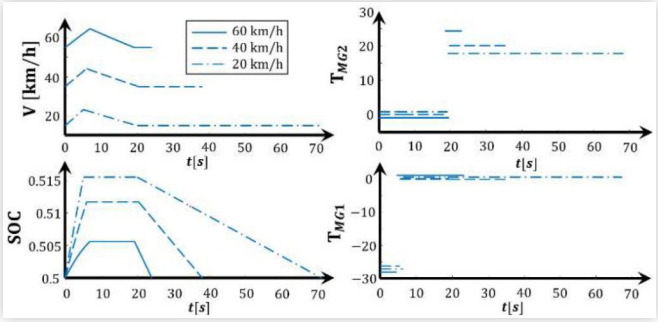

TABLE 2 Power flow within PSD of the constant speed strategy

		Charge Phase			Discharge Phase	
Case	P_{req} (kw)	P_{eng} (kw)	P_{MG1} (kw)	P_{wheels} (kw)	P_{MG2} (kw)	P_{wheels} (kw)
20 km/h	1.38	5.02	−3.65	1.38	1.38	1.38
40 km/h	3.18	5.94	−2.76	3.18	3.18	3.18
60 km/h	5.84	7.28	−1.44	5.84	5.84	5.84

-Convention:

For MGs: $P > 0$ for driving and $P < 0$ for generating.

TABLE 3 Power flow within PSD of the three-phase strategy

		Pulse Phase			Discharge Phase	
Case	P_{req} (kw)	P_{eng} (kw)	P_{MG1} (kw)	P_{wheels} (kw)	P_{MG2} (kw)	P_{wheels} (kw)
20 km/h	1.38	17.95	−13.65	4.30	1.01	1.01
40 km/h	3.18	19.12	−9.46	9.66	2.67	2.67
60 km/h	5.84	20.47	−4.36	16.12	5.08	5.08

-Convention:

For MGs: $P > 0$ for driving and $P < 0$ for generating.

is solely driven by MG 2. At that time, vehicle speed remains stable while battery SoC gradually declines to the initial value. The idea of Constant Speed Strategy is very similar to the thermostatic strategy in series HEVs; the optimization results are shown in Figure 6; and its power distribution of the samples are outlined in Table 2.

In the scenarios of 20 km/h, 40 km/h and 60 km/h, the optimized fuel consumptions per 100 km of the constant speed strategy are 5.22 L, 4.83 L and 5.07 L respectively.

Three-Phase Strategy

Under the three sample speeds, the optimized speed, SoC profiles and power distribution of the three-phase strategy are shown in Figure 7 and Table 3. The vehicle first accelerates from the lower speed V_{min} to the higher speed V_{max}, then glides from the higher speed V_{max} to the initial speed V_{min}, followed by a constant speed phase with a fixed speed of V_{min}. As the engine torque output is basically stable at different average cruising speeds, the higher average cruising speed leads to a smaller acceleration, so that it takes longer to achieve the same ΔV. In the glide phase, with the average speed increasing, the resistance of the vehicle increases gradually, therefore the deceleration is higher, which leads to a shorter deceleration time. Due to the lower speed of the last phase, the real average speed is slightly lower than the predefined value within a single cycle.

The battery SoC first increase from initial value SOC_0 to a higher value SOC_f in the pulse phase. In the glide phase, because of both two electric motors are not operating, SoC keeps stable at the value SOC_f. As MG 2 starts to operate in the drive mode, SoC decreases to its initial value SOC_0 in the last phase.

At the sample speeds of 20 km/h, 40 km/h and 60 km/h, the fuel consumptions per 100 km of the three-phase strategy are 3.26 L, 3.12 L and 3.63 L, respectively.

If the fuel-saving rate is defined as:

$$\xi = \frac{F_{CSS} - F_{PCS}}{F_{CSS}} \tag{22}$$

where F_{CSS} represents fuel consumption of the constant speed strategy, and F_{PCS} is the fuel consumption of the periodic cruising strategy.

Compared with the constant speed strategy, the fuel-saving rates of the three-phase strategy are 38.5%, 36.2% and 28.9% respectively.

Two-Phase Strategy

Since the three-phase cruising strategy consists of two switches in a single cycle, leads to more complex control rules. And due to the existence of the third phase, the average speed of the three-phase strategy is slightly less than the predefined value.

If the last two phases of the three-phase can be merged into one phase, that is, the battery SoC and the vehicle speed both decline simultaneously, the control complexity can be reduced by a certain degree, and the actual average speed can approximately equal to the preset value.

The vehicle speed and battery SoC profiles of the two-phase strategy under three sample speeds can be seen in Figure 8. The observed change of vehicle speed and battery SoC during the pulse phase are almost same as the three-phase

FIGURE 8 Optimization results of two-phase strategy under sample speeds

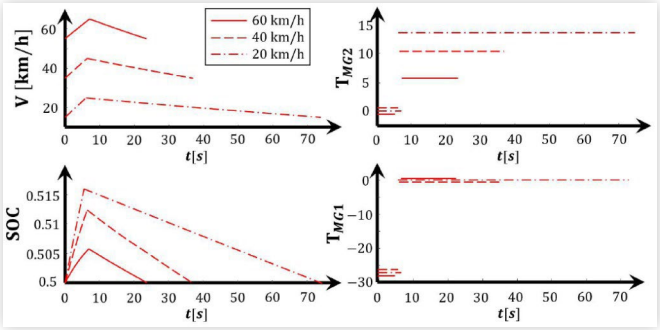

TABLE 4 Power flow within PSD of the two-phase strategy

		Pulse Phase			Glide(Discharge) Phase	
Case	P_{req} (kw)	P_{eng} (kw)	P_{MG1} (kw)	P_{wheels} (kw)	P_{MG2} (kw)	P_{wheels} (kw)
20 km/h	1.38	18.22	−13.76	4.46	0.44	0.44
40 km/h	3.18	19.30	−9.60	9.70	1.56	1.56
60 km/h	5.84	20.51	−4.26	16.25	3.06	3.06

-Convention:

For MGs: $P > 0$ for driving and $P < 0$ for generating.

strategy. However, there is a difference occurring in the following phase, where the vehicle speed and the battery SoC simultaneously decline to their initial values. MG 1 functions as a generator in pulse phase, and shuts down in the glide(discharge) phase. MG 2 does not operate in the pulse phase, and only provides a relatively small torque to prolong the glide phase. Therefore, battery energy is consumed, and both speed and SoC declines.

The fuel consumption under three sample speeds of the two-phase strategy are 3.30 L, 3.26 L and 3.72 L, respectively. Compared with the constant speed strategy, the fuel-saving rates of the two-phase strategy are 36.4%, 32.5% and 26.6% respectively. Furthermore, the fuel economy of the two-phase strategy is slightly worse than the three-phase strategy.

Mechanism Analysis

The fuel consumption and fuel-saving rate of the periodic strategies and constant speed strategy under different average cruising speeds are shown in Figure 9.

Two conclusions can be drawn from the Figure 9: 1). The fuel economy of two periodic strategies are far better than the constant speed strategy, but the fuel-saving rate becomes marginal as the speed increases; 2). The fuel economy of the three-phase strategy is slightly better than the two-phase strategy, and the difference between them first increased and then decreased.

The engine operation points of the periodic strategies and constant speed strategy are shown in Figure 10.

FIGURE 9 The fuel consumptions and fuel-saving rates under different average cruising speeds

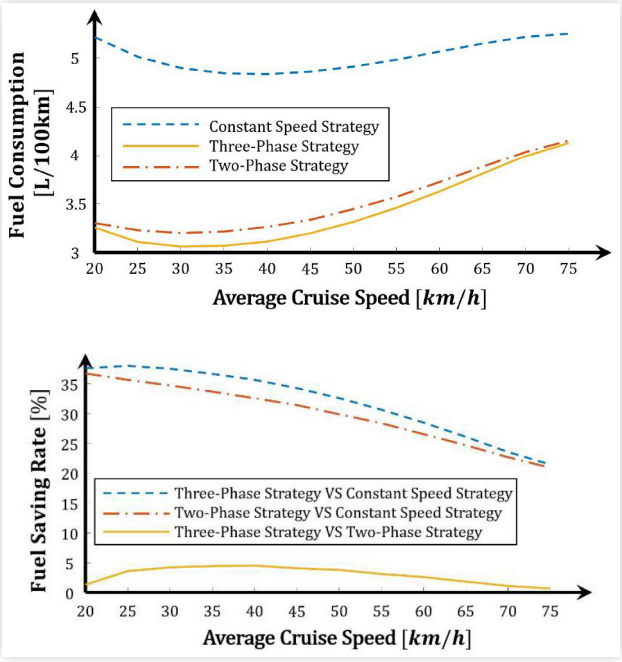

FIGURE 10 The distribution of the engine operation points of the periodic strategies and constant speed strategy

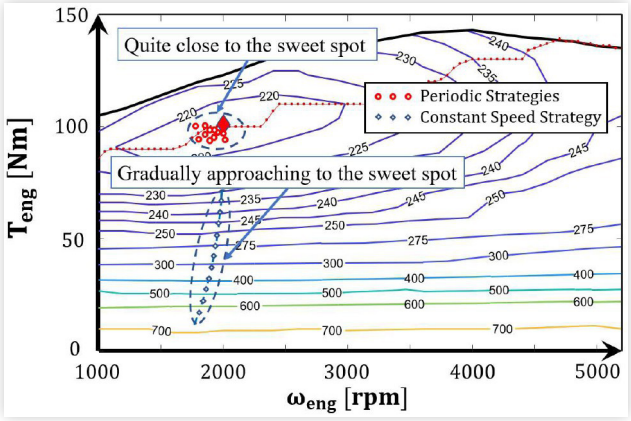

As shown above, the engine operation points of both periodic strategies are quite close to the sweet spot, and almost kept stable at different average speeds. However, the engine operation points of the constant speed strategy are gradually close to the optimal efficiency region as cruising speed increases. The lower the average speed, the further it deviates away from the sweet spot.

Based on the two phenomena above, this section will focus on the fuel-saving mechanism of the periodic strategies by explaining the answering following two questions:

1. Why is the fuel economy of the periodic cruising strategy better than constant speed strategy under the same average cruise speed?
2. Why is the fuel economy of the three-phase strategy better than two-phase strategy under the same average cruise speed?

For question 1, because the power of the sweet point is far greater than the required power when vehicle is cruising at a medium-low speed, the extra engine power can be stored in vehicle body and battery in the form of kinetic energy and electric energy. Taking the parameters in this paper as an example, when vehicle cruises at 40 km/h, the required power is about 3.18 kw, while the engine power of the constant speed strategy is only 5.96 kw, which is far below the power of sweet spot (20.94 kw).

Under the constant speed scenarios, the engine operation points are constrained by the PSD torque balance, thus the engine torque output cannot be too high; otherwise, vehicle speed and(or) engine speed will change, which can deteriorate the power source efficiency. This characteristic severely restricts the location of the engine operation points, resulting in a deviation from the optimal efficiency region, especially in medium and low speed scenarios.

In the periodic cruising strategies, the engine torque is large enough to pulse the vehicle, and the extra energy can be stored in the vehicle body mass as the form of kinetic energy, while maintaining the engine operation point close to the sweet spot, as shown in Figure 10. Furthermore, there is a trade-off between MG efficiency and engine efficiency, so the engine operation points are not coinciding with the sweet spot completely.

For question 2, because the pulse (charging) phases of two periodic strategies are basically the same, the difference in fuel economy between the two periodic strategies mainly caused by differences in the latter phases. In general, different periodic strategy has different means of discharge, leading to a difference between MG efficiencies.

The fundamental difference between the three-phase strategy and two-phase strategy is that MG 2 in the three-phase strategy provides a full load in its glide phase, while it can only provide a partial load in two-phase strategy. Under the same cruising speed (i.e., same MG 2 speed), the difference between two types of the MG 2 operations can be seen in Figure 11. The operation points of the three-phase strategy are above the two-phase strategy.

FIGURE 11 MG 2 operation points of the three-phase strategy and two-phase strategy

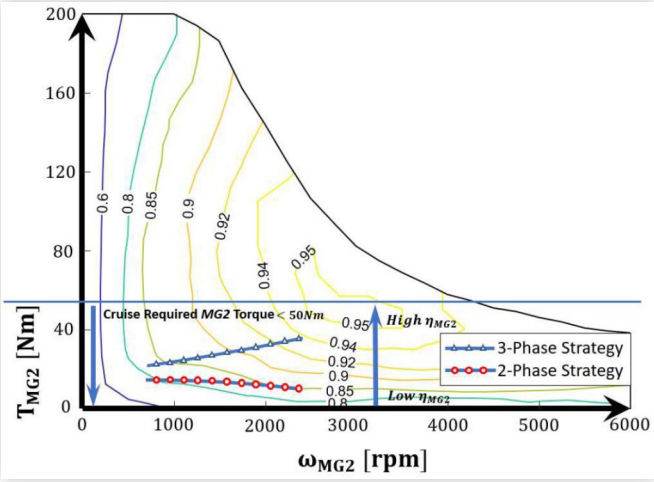

Additionally, the operation points of three-phase strategy demonstrated a higher efficiency under the same MG 2 speed, as shown in Figure 11. Therefore, there is a difference between the two periodic strategies. Due to the higher efficiency of the three-phase strategy, the vehicle can travel longer distances. In the non-plug-in HEVs, the electricity stored in the battery eventually comes from gasoline. Therefore, a higher motor efficiency can produce a better fuel economy, which means the fuel economy of the three-phase strategy is better than the two-phase strategy considering the change of initial/final SoC.

It should be noted that the order of the last two phases of the three-phase strategy can be swapped, i.e., the battery SoC can first go down, then followed by a vehicle speed decrease, which is also feasible.

In general, each of the two periodic cruising strategies has its own inherent benefits and drawbacks. Although the two both can achieve a significant improvement on fuel economy compared with constant speed strategy. While the three-phase strategy can attain the better fuel economy, the control complexity of the two-phase strategy is lower than that of the three-phase strategy.

Conclusions

This paper analyses the periodic strategies of the PS-HEV. Two strategies are proposed, and their optimal operations can be identified by an optimization problem based on mechanical structure analysis. Therefore, a PS-HEV's periodic cruising problem is constructed and solved by SNOPT. Comparing with constant speed strategy, the main findings are as follows:

1. The periodic strategies can make full use of the engine power; thus, it is easy to adjust the engine operation points to be close to the sweet spot. Due to the fact that the constant speed strategy is constrained by the system torque balance, its engine operation points cannot reach the sweet spot, especially in medium-low speed. However, the periodic strategies have speed fluctuations, leading to a less comfortable ride.
2. Due to the characteristics of the MG efficiency, a larger torque results in a greater efficiency within the range of the cruising torque required under the same MG speed. Therefore, the fuel economy of the three-phase strategy that provides full load is better than that of the two-phase strategy that only provides partial load;

In terms of simple control rules and good real-time performance, periodic strategies have the potential to be applied onto production vehicles in the future, such as ACC system. However, due to the speed fluctuation, it is generally not suitable for high traffic density scenarios. On the other hand, the good fuel-saving effect of the periodic control is based on the precise control of the power sources. Therefore, autonomous vehicles are ideal platforms for periodic control strategies. However, for PS-HEVs using periodic strategies, fuel economy in car-following and high-speed scenarios is yet to be studied.

References

1. Zhang, X., Li, S.E., Peng, H., and Sun, J., "Efficient Exhaustive Search of Power Split Hybrid Powertrains with Multiple Planetary Gears and Clutches," *ASME-Journal of Dynamic Systems, Measurement and Control* 137(12):1-12, 2015, doi:10.1115/1.4031533.
2. Zhang, X., Li, S.E., Peng, H., and Sun, J., "Design of Multimode Power Split Hybrid Vehicles-A Case Study on the Voltec Powertrain System," *IEEE Transactions on Vehicular Technology* 65(6):4790-4801, 2016, doi:10.1109/TVT.2016.2531740.
3. Sciarretta, A. and Guzzella, L., "Control of Hybrid Electric Vehicles," *Control Systems IEEE* 27(2):60-70, 2007, doi:10.1109/MCS.2007.338280.
4. Mansour, C. and Clodic, D., "Dynamic Modeling of the Electro-Mechanical Configuration of the Toyota Hybrid System Series/Parallel Power Train," *International Journal of Automotive Technology* 13(1):143-166, 2012, doi:10.1007/s12239-012-0013-8.
5. Li, S.E., Hu, X., Li, K., and Ahn, C., "Mechanism of Vehicular Periodic Operation for Optimal Fuel Economy in Free-Driving Scenarios," *Intelligent Transport Systems IET* 9(3):306-313, 2015, doi:10.1049/iet-its.2014.0002.
6. Li, S.E., Peng, H., Li, K., and Wang, J., "Minimum Fuel Control Strategy in Automated Car-Following Scenarios," *IEEE Transactions on Vehicular Technology* 61(3):998-1007, 2012, doi:10.1109/TVT.2012.2183401.
7. Xu, S., Li, S.E., Zhang, X., Cheng, B. et al., "Fuel-Optimal Cruising Strategy for Road Vehicles with Step-Gear Mechanical Transmission," *IEEE Transactions on Intelligent Transportation Systems* 16(6):3496-3507, 2015, doi:10.1109/TITS.2015.2459722.
8. Xu, S., Li, S.E., Peng, H., Cheng, B. et al., "Fuel-Saving Cruising Strategies for Parallel HEVs," *IEEE Transactions on Vehicular Technology* 65(6):4676-4686, 2016, doi:10.1109/TVT.2015.2490101.
9. Li, S.E., Li, R., Wang, J., Hu, X. et al., "Stabilizing Periodic Control of Automated Vehicle Platoon with Minimized Fuel Consumption," *IEEE Transactions on Transportation Electrification* 3(1):259-271, 2017, doi:10.1109/TTE.2016.2628823.
10. Li, S.E., Deng, K., Zheng, Y., and Peng, H., "Effect of Pulse-And-Glide Strategy on Traffic Flow for a Platoon of Mixed Automated and Manually Driven Vehicles," *Computer-Aided Civil and Infrastructure Engineering* 30(11):892-905, 2015, doi:10.1111/mice.12168.
11. Liu, J. and Peng, H., "Modeling and Control of a Power-Split Hybrid Vehicle," *IEEE Transactions on Control Systems Technology* 16(6):1242-1251, 2008, doi:10.1109/TCST.2008.919447.
12. Zhang, X., Li, C.-T., Kum, D., and Peng, H., "Prius+ and Volt-: Configuration Analysis of Power-Split Hybrid Vehicles with a Single Planetary Gear," *IEEE Transactions on Vehicular Technology* 61(8):3544-3552, 2012, doi:10.1109/TVT.2012.2208210.
13. Gill, P.E., Murray, W., and Saunders, M.A., "SNOPT: An SQP Algorithm for Large-Scale Constrained Optimization," *SIAM Review* 47(1):99-131, 2005, doi:10.1137/S0036144504446096.

Contact Information

Prof. Qingfeng Lin
School of Transportation Science and Engineering
Beihang University, Beijing, China
linqf@buaa.edu.cn

Xuedong Liu
School of Transportation Science and Engineering
Beihang University, Beijing, China
buaalxd@foxmail.com

Xiaoxue Zhang
College of Engineering
China Agricultural University, Beijing, China
zxxkybl@126.com

Zhitao Wang
Department of Automotive Engineering
Tsinghua University, Beijing, China
wangzt16@mails.tsinghua.edu.cn

Shaobing Xu
Department of Mechanical Engineering
University of Michigan, Ann Arbor, USA
xushao@umich.edu

Prof. Shengbo Li
Department of Automotive Engineering
Tsinghua University, Beijing, China
lishbo@tsinghua.edu.cn

Acknowledgments

This study is supported by NSF China with 51575293 and 51622504, National Key R&D Program of China with 2016YFB0100906, and International Sci&Tech Cooperation Program of China under 2016YFE0102200.

Definitions/Abbreviations

ACC - Adaptive Cruise Control

BSFC - Brake Specific Fuel Consumption

CS - Constant Speed strategy

CVT - Continuous Variable Transmission

ICE - Internal Combustion Engine

MG - Motor-Generator

PnG - Pulse and Glide

PSD - Power-Split Device

SoC - State of Charge

SQP - Sequence Quadratic Programming

ISSN 0148-7191